Radiometric normalization of remotely sensed images: a new approach using linear scattergram regression

Hafez Abbas Afify

Transporation Eng. Dept., Faculty of Eng., Tanta University, Tanta, Egypt

This paper is devoted to introduce and evaluate a suggested new empirical method for radiometric normalization of multitemporal remotely sensed images based on the Linear Scattergram Regression (LSR). The aim is to produce radiometrically comparable multispectral images in a way that pixel values from one image carry the same or, at least, similar meaning as pixel values from another. The LSR procedure utilizes the scattergram of the reference image versus the subject image to assign the locations of the unchanged pixels between both images. Then, only the gray level values of these unchanged pixels are used to derive the gain and offset of the LSR required for each band. To evaluate its performance, the LSR procedure was compared with three traditional empirical methods namely; histogram matching, image regression, and statistical normalization. The analysis of the resulted normalized images using these methods revealed that the accuracy obtained from using the LSR procedure is the highest of all methods.

في هذا البحث تم تقديم و تقييم أسلوب جديد (LSR) للمعالجة الطيفية لصور الاستشعار عن بعد المكتسبة لنفس المنطقة ولكن في اوقــات مخـتلفة وتحـت ظروف بيئية متباينة، حيث يكون الغرض من الدراسة هو جعل الخلايا المتناظرة في الصور المختلفة تحتوي كلما امكن على نفس درجة الانعكاسية. يعتمد أسلوب (LSR) على شكل انتشار الخلايا تبعا لدرجة انعكاسيتها بين صورة المرجع و الصورة المراد معالجتها (الاسكاترجرام). ويتم ذلك بتحديد مواقع الخلايا التي اختلفت درجة انعكاسيتها في الصــورتين نتـيجة لاختلاف العوامل البيئية مثل درجة تشتت و امتصاص الغلاف الجوي و درجة الرطوبة في اوقات الرصــد المختلفة وليس نتيجة لاختلاف المعالم الارضية المصورة في هذه الخلايا، ثم تستخدم هذه الخلايا فقط لاشتقاق معادلة الـتحويل الخطـية التـي تطـبق على كل خلية في الصورة المراد معالجتها للحصول على الصورة المشابهة طيفيا لصورة المـرجع.كمــا تــم عمل دراسة مقارنة بين هذه الطريقة الجديدة (LSR) و ثلاث من الطرق المألوفة الاستخدام وهي طريقة تشــابه الهستوجرام، و طريقة المعادلة الخطية للصورة و طريقة المعالجة الاحصائية حيث اثبت الدراسة ان طريقة (LSR) تعطي صورة معالجة بدرجة دقة اعلى من تلك الناتجة باستخدام أى من الطرق الثلاث الأخرى.

Keywords: Multitemporal images, Radiometric normalization, Scattergram regression, Histogram matching

1. Introduction

Many projects involve the use of more than one image. For example, it is often desirable to generate mosaics of images taken at different times, or to detect the changes in the reflectance of ground features at different times and locations. Digital number differences between the corresponding unchanged pixels of the multitemporal data set are encountered. These differences are not related to the reflectance of the land surface, but they are resulted from the variation of solar illumination conditions, atmospheric conditions, viewing geometry, and sensor system response at different acquisition times. Therefore, it is essential to minimize these differ-

ences by radiometric normalization before extracting information from multitemporal data, so that the pixels of the subject image would take the same or close gray level values as the corresponding pixels of the reference image.

Radiometric normalization can be carried out based on modeling the physical environment or on empirical adjustment using scene comparisons. However, since the necessary environmental data required for physical correction such as atmospheric scattering and absorption conditions, visibility, and humidity at acquisition time are often difficult or impossible to obtain [1], and also highly detailed corrections may not be necessary [2], it is recommended and preferred to use the procedures of empirical adjustment to radiomet-

rically normalize multidate remotely sensed images.

The purpose of this paper is to describe and evaluate a proposed empirical radiometric normalization technique. The new approach utilizes the scattergram of the reference image versus the subject image to identify the locations of no-change pixels in the two images. These no-change pixels are then used to determine the gain and offset of the Linear Scattergram Regression (LSR) required for transforming each band of the subject image. The study also involves a comparison between the LSR technique and three most commonly used procedures namely; histogram matching, image regression, and statistical normalization. Thus the performance and reliability of the LSR technique are evaluated.

2. Empirical radiometric normalization techniques

Empirical radiometric normalization techniques are based on the observation of certain radiometric characteristics in both the subject and the reference images. Then, a formula, based on the observed radiometric characteristics, is established and applied to the digital number values of the subject image to produce a new (normalized) image whose digital number values are radiometrically matching those of the reference image. Three of the widely used techniques are as follows.

2.1. Histogram matching

In this method, the cumulative histograms of the subject and the reference images are first determined, and the cumulative density function of each image is then calculated. Histogram matching technique normalizes the subject image to the reference image by relating the cumulative density functions of both images to each other according to the formula [1]:

$$DN_N = (P_R)^{-1} [P_S (DN_S)],$$

where:
DN_N = the normalized digital number of a pixel,

$(P_R)^{-1}$= the inverse cumulative density function of the reference image,
P_S = the cumulative density function of the subject image, and
DN_S = the digital number of a pixel in the subject image.

The process of histogram matching is best looked at as consisting of two steps, first is to equalize the histogram of the subject image, and second is to normalize the equalized histogram of the subject image to the histogram of the reference image [3].

2.2. Image regression

This technique relates the digital numbers of whole or corresponding subsets of the subject and reference images through a simple linear regression equation of the form:

$$DN_N = a + b (DN_S),$$

where:
DN_N, and DN_S = the digital number of the normalized and subject images, and
a, and b= the offset and the gain of the linear regression.

The subsets are selected as pairs, one from each image. These pairs are chosen considering that any digital number differences in the corresponding pixels is referred to different illumination, atmospheric, and sensor response conditions at images acquisition times and is not related to any change in the land surface. The equation is applied first using the digital number of the reference image to determine the unknown parameters (a, and b), and then applied again to each pixel of the subject image to generate the normalized image.

2.3. Statistical normalization

This technique is based on matching the mean and the standard deviation of the subject and reference images according to the formula:

$$(DN_N - M_R) / \sigma_R = (DN_S - M_S) / \sigma_S ,$$

where:

DN_N = the normalized digital number of a pixel,

M_R, and M_S = the mean of the reference and subject images, respectively,

σ_R, and σ_S = the standard deviation of the reference and subject images, and

DN_S = the digital number of the subject image [3].

2.4. *The new approach: linear scattergram regression*

A scattergram is a two dimensional histogram that provides the number of pixels which have two specific gray level values (one in each image). This technique employs the scattergram of similar bands in both the subject and reference images to determine the position of the pixels where no change had occurred in both images. These no-change pixels are then used to derive the gain and offset of the linear regression for each spectral band.

The details of application of all methods and a comparative study will be demonstrated through a case study in the following sections

3. Study area

The image data used to compare different techniques of radiometric normalization were two 400 x 400 pixel subscenes cut out of an overlapping area of two SPOT multispectral images acquired on September 26, 1991 and, June 18, 1997.

SPOT 1991 data is cloud free while some cloud covers are found in SPOT 1997 data. They concentrate in the subscene center and spread slightly to the lower left corner. The area under investigation covers the middle part of Alexandria city, Egypt. The area is characterized by the presence of urban areas in the upper left corner, water bodies with some aquatic vegetation in the lower left side. Al-Nuzhah airport is found in the upper right side with some cultivated areas in the south as shown in fig. 1.

4. Data processing

The 1991 image was selected as the reference image for geometric registration. Fourteen ground control points were used to tie down the 1997 image (the subject image) to the reference image with resampling based on the nearest neighbor interpolation routine. The standard deviations were 0.26 pixel in X-direction and 0.23 pixel in Y-direction. After registration, the subscenes were cut out from the images and the cloud pixels in 1997.

1991 image   1997 image

Fig. 1. The study area .

subscene were masked out using a threshold of visual bands. Different modules of the PCI image-processing software were used to process the data at the steps of this research. The radiometric characteristics of 1991 and 1997 subscenes are summarized in table 1.

Table 1
Radiometric properties of original and normalized images

Image	Band	Min.	Max.	Mean	Standard dev.
Original 1991	1	41	176	63.25	11.37
	2	30	189	57.48	15.50
	3	21	161	66.32	20.74
Original 1997	1	47	254	80.41	26.85
	2	41	254	88.60	32.88
	3	30	254	105.84	31.20
Histogram matching	1	44	176	63.66	12.43
	2	31	189	58.14	17.79
	3	21	161	66.83	21.10
Image regression	1	57	90	62.37	4.31
	2	47	89	56.32	6.56
	3	41	113	65.39	9.98
Statistical normaliza-tion	1	48	136	62.50	11.37
	2	34	134	56.24	15.47
	3	14	163	64.89	20.79
LSR	1	47	169	66.93	15.84
	2	35	156	62.02	18.73
	3	21	160	68.13	19.34

Figs. 2, 3, and 4 represent the scattergrams of bands 1, 2 and 3 of the SPOT images, respectively. The elements with largest number of pixels are shown in white color (center of the cluster) surrounded by light to dark gray, and black color elements. The darker gray of a scattergram element means a smaller number of pixels occupies this element.

Referring to the scattergram figures, it can be noted that:
1. The minimum gray level values in 1997 data for the three bands are greater than the corresponding values in 1991 data which is an indication that 1997 data had more haze than 1991 data.
2. The shift of the lower left corner of the scattergrams from the origin is larger for shorter wavelengths. This means that the effect of atmospheric scattering is greater for shorter wavelengths.
3. Each of the scattergrams of band 1, and 2 shows a single dense data cluster (area of light

gray shadow). This single cluster contains water and land surface pixels.
4. The scattergram of band 3 (infrared band) shows two separate clusters for water and land surface pixels. The small cluster close to the origin represents the water pixels while the large one in the middle of the scattergram represents the land surface pixels. This scattergram will be considered to describe the LSR technique although the scattergrams of visual bands could have been used.
5. Inside each cluster, the element that carries the maximum number of pixels is known as the cluster center. In fig. 4, the water cluster center is (38,26) with 182 pixels, and the land surface cluster center is (98,65) with 561 pixels. Elvidge et al. [4] developed a scattergram regression in which the centers of the water and land clusters of the infrared band were used to determine the initial gain and offset of the linear relationship between the subject and reference images [4].

After determining the cluster centers of the infrared scattergram, the regions of no-change are defined using a rectangular window for each cluster. The rectangular window is centered at the cluster center and has dimensions depending on the cluster extension and shape. In this study, dimensions of the water window is defined to be (±8, ±5) cells from the water cluster center (38, 26), and dimensions of the land surface window is (±15, ±10) cells from the land cluster center (98, 65) respectively. Table 2 summarizes the properties of the water and land rectangular windows.

This means that we are looking for the unchanged water pixels, which have gray levels ranging from 30 to 46 in 1997 data, and have gray levels ranging from 21 to 31 in 1991 data. We are also looking for the unchanged land surface pixels, which have gray levels ranging from 83 to 113 in 1997 data and have gray levels ranging from 55 to 75 in 1991 data.

The locations of the no-change land surface pixels were determined as follow:
1. Image 1997 was thresholded using DN range from 83 to 113 resulting in an image mask involving the location of the pixels whose scattergram elements lie inside strip A, see fig. 4.
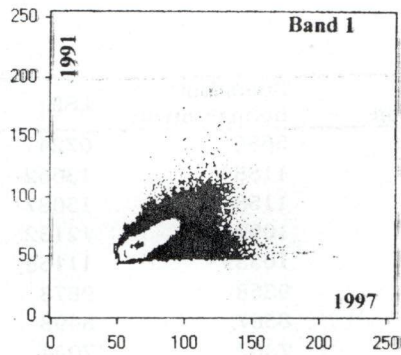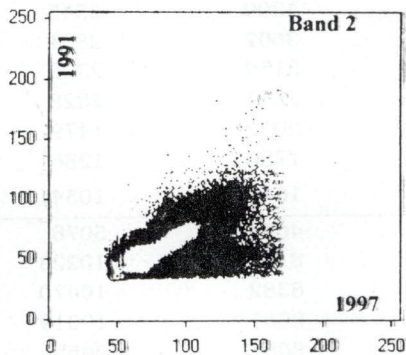
Fig. 2. Scattergram of band 1.
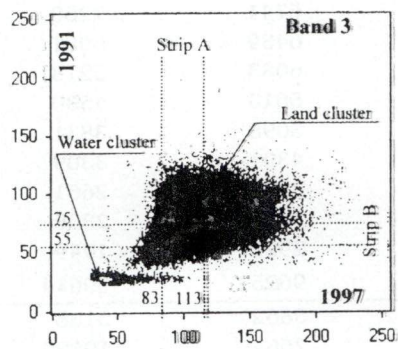

Fig. 3. Scattergram of band 2.

Fig. 4. Scattergram of band 3.

Table 2
Properties of the water and land rectangular windows

Cluster center	Window size from center	Window dimension	Digital numbers at window boundary	Number of pixels
Water cluster	38, 26	±8, ±5	7 x 11	0-46, 1-31	116
Land cluster	98, 65	±15, ±10	1 x 21	3-113, 55-75	4914

2. Image 1991 was thresholded using DN range from 55 to 75 resulting in another image mask involving the location of the pixels whose scattergram elements lie inside strip B.

3. The logical AND was applied to the two image masks resulting in a new image mask containing the location of the pixels whose scattergram elements lie inside both strip A and strip B. In other words, inside the rectangular window of the land surface cluster.

The same steps were applied to locate the unchanged water pixels. Then, the logical OR was applied to the two image masks containing both the unchanged land surface and water pixels to assign the final set of unchanged pixels between both images. This final set was used to derive the gain and offset of the LSR technique.

5. Results and analysis

1997 subscene was radiometrically normalized to 1991 subscene using the three methods described before in addition to using the LSR method. The radiometric properties of the normalized images are summarized in table 1 Accuracy of each of the four normalized images were evaluated as follow:

1. The reference image was subtracted from the normalized image, pixel by pixel, resulting in an error image.

2. The histogram of the error image was generated, and the pixels whose absolute error values equal to 1, 2, 3,..., up to 15 were counted.

3. These numbers of pixels according to their absolute error values are shown in table 3, and presented graphically for different bands in figs. 5, 6, and 7.

As shown in table 1 significant differences between similar radiometric properties of 1991 and 1997 images have been founded. These differences are not related to the change of the land surface but they are caused by the variation of illumination, atmospheric, and sensor conditions at different acquisition times. Except for the standard deviation, Histogram matching method provided a normalized subscene with very close radiometric characteristics as the reference subscene.

Table 3
Number of pixels according to their absolute error values

| Band No.	Absolute Error value	Histogram matching	Image regression	Statistical normalization	LSR
(1)	0	6446	5346	5686	6724
	1	12599	10294	11884	13662
	2	12395	10091	11581	13087
	3	11523	9789	10924	12132
	4	10582	9584	10359	11158
	5	9523	9040	9368	9878
	6	8194	8018	8567	8498
	7	7032	7729	7307	7094
	8	6164	6677	6295	5514
	9	4516	6110	5346	4405
	10	3668	5524	4399	3545
	11	3074	4436	3602	2801
	12	2569	3940	3150	2320
	13	2208	3314	2564	1828
	14	1777	2602	2092	1479
	15	1377	2071	1756	1286
	Total	103647	104565	104880	105411
(2)	0	4727	3796	4094	5078
	1	9216	7728	8116	10223
	2	9186	7439	8382	10470
	3	8910	7375	8261	10019
	4	8715	7131	8087	9455
	5	8155	6661	7601	8954
	6	7579	6456	7097	8268
	7	7029	6544	6741	7260
	8	6240	6220	6439	6081
	9	5706	5780	6083	5218
	10	5111	5377	5610	4530
	11	4613	5303	5098	3831
	12	3943	5230	4391	3309
	13	3473	5130	3971	2661
	14	3027	5156	3354	2308
	15	2453	4672	2928	1949
	Total	98083	95998	96253	99614
(3)	0	5367	3891	3862	5158
	1	9626	7367	7562	10120
	2	8164	7630	7667	9499
	3	7390	7315	7383	8780
	4	7036	7097	7535	8127
	5	6922	6633	7376	7178
	6	6309	5998	7322	6548
	7	5479	5633	6434	6046
	8	4912	5376	5846	5310
	9	4404	4685	5234	4570
	10	4072	4377	4458	4080
	11	3649	4048	4176	3615
	12	3305	3582	3626	3204
	13	3010	3359	3370	2942
	14	2928	3112	3040	2603
	15	2646	2848	2724	2253
	Total	85219	82951	87615	90033
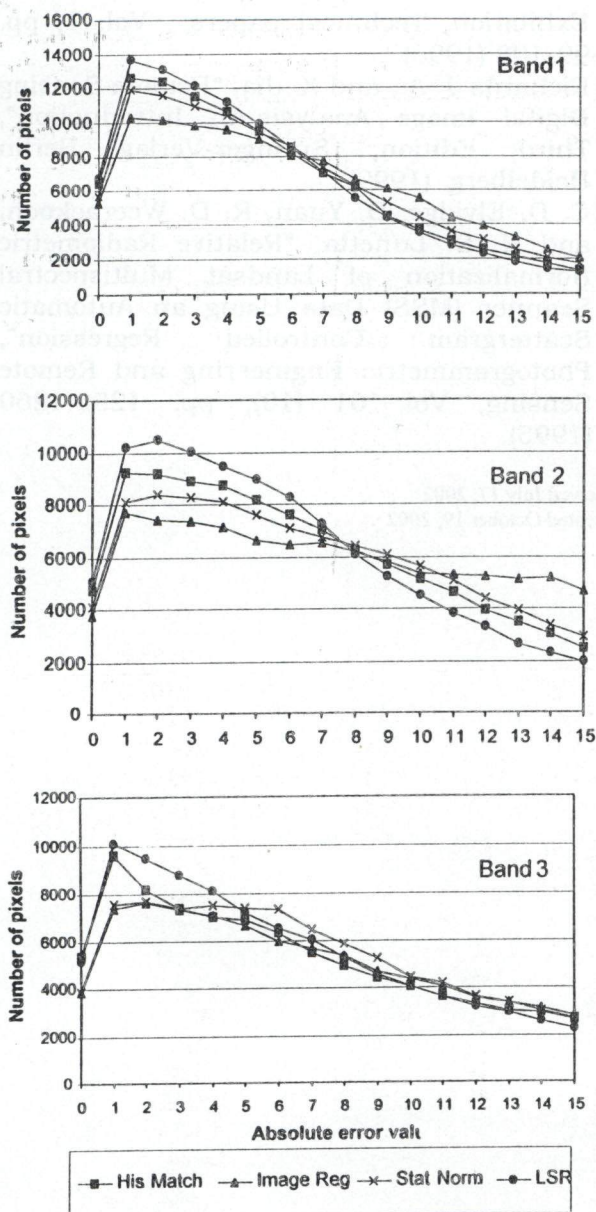
Fig. 5, 6, and 7. Number of pixels according to their absolute error values. (Bands 1,2, and 3, respectively).

The drawback of the Image regression and Statistical normalization techniques is that, they deal with all the image pixels without cleaning from cloud, shadow, or even changed pixels which biased the resulted pixel to pixel relationship. The normalized subscene resulted using statistical normalization technique has the same standard deviation and almost the same mean values as the reference subscene.

The graphical representation of the absolute error values in figs. 5, 6, and 7 indicated that, the numbers of pixels, which have low absolute error values (from 0 to 6 for band 1, from 0 to 7 for band 2, and from 0 to 5 for band 3) are the greatest when using the LSR method rather than when using any of the other three methods.

Inversely, since the same total number of pixels was examined by the four methods, the numbers of pixels, which have high absolute error values, (from 7 to 15 for band 1, from 8 to 15 for band 2, and from 6 to 15 for band 3) are the least when the LSR method was used.

Moreover, the total number of pixels, having absolute error values equal to or less than 15 is the greatest when using the LSR method. As shown in table 3, these total numbers are 105411 pixels for band 1, 99614 pixels for band 2, and 90033 pixels for band 3.

6. Conclusions

A proposed Linear Scattergram Regression (LSR) technique has been introduced for performing radiometric normalization of multitemporal remote sensing images. Compared with the three widely used radiometric normalization methods, the LSR method provided the highest accuracy. This is because the LSR involves first of all a computer-based procedure for identification of the no-change pixels in both images. Then, the transformation formula is derived based only on these no-change pixels. Moreover, the LSR method has improved the accuracy of the normalized image since it avoids the contribution of the cloud, shadow, and changed pixels in deriving the offset and gain of the transformation formula.

Not only the infrared band but also any of the visual bands can be employed by the LSR method to locate the positions of the no-change pixels.

The graphical representation of the results, showed that the highest accuracy has been provided by the LSR method (the largest numbers of pixels at low absolute error values, and the smallest numbers of pixels at high absolute error values). Histogram Matching and the Statistical Normalization methods

followed the LSR method, and the Image Regression method has provided the least accurate normalized image.

References

[1] T. M. Jeffrey D. Xiaolong, H. Cheshire, S. Khorram, "Comparing Empirical Normalization Methods for a Mosaic of Landsat Thematic Mapper Data", ASPRS / ACSM Annual Convention and Exhibition, Technical papers, Vol. 1, pp. 251-260 (1996).

[2] P. F., W. K. Houhoulis Michener, and J. W. Jones, "Detection of Vegetation Changes Associated with Tropical Storm Alberto in a Longleaf Pine-Wiregrass Ecosystem", ASPRS / ACSM Annual Convention and Exhibition, Technical papers, Vol. 1, pp. 99-108 (1996).

[3] Richards J. A., and X. Jia, "Remote Sensing Digital Image Analysis-An Introduction", Third Edition, Springer-Verlag Berlin Heidelberg (1999).

[4] C. D. Elvidge, D. Yuan, R. D. Weerackoon, and R. S. Lunetta, "Relative Radiometric Normalization of Landsat Multispectral Scanner (MSS) Data Using an Automatic Scattergram Controlled Regression", Photogrammetric Engineering and Remote Sensing, Vol. 61 (10), pp. 1255-1260 (1995).